This journal is © The Owner Societies 2013

Supporting information for:

Solvatochromism of pyranine-derived photoacids

Christian Spies[#], *Björn Finkler*[#], *Nursel Acar*[§], *Gregor Jung*[#]*

[#]Biophysical Chemistry, Saarland University, Campus, Building B2 2, D-66123 Saarbrücken, Germany

[§]Ege University, Faculty of Science, Department of Chemistry, 35100 Bornova, Izmir, Turkey

Synthesis of Trisodium-8-methoxypyrene-1,3,6-trisulfonate (MPTS)

Trisodium-8-hydroxypyrene-1,3,6-trisulfonate (2.09 g, 4.0 mmol) was dissolved in 80 mL anhydrous DMSO. After addition of sodium hydroxide (0.160 g, 4.1 mmol), the mixture was stirred for 30 minutes at room temperature. Methyl iodide (0.710 g, 5.0 mmol) was added and the resulting solution was stirred for 48 hours at room temperature. Solvent and excess methyl iodide were removed in vacuo. The yellow residue was suspended in 50 ml ethylacetate and filtered. After the filter cake was washed with ethylacetate (2 × 50 mL) and acetone (3 × 50 mL) and dried under vacuum, the crude product was recrystallized from methanol/water. The sodium-salt of **MPTS** was isolated as yellow powder (1.90 g, 88%).

^{1}H-NMR (400MHz, DMSO-d6): δ = 9.12 (1H, d, ^3J (H,H) = 10Hz), 9.04 (1H, d, ^3J (H,H) = 10Hz), 9.02 (1H, s), 8.95 (1H, d, ^3J (H,H) = 10Hz), 8.37 (1H, d, ^3J (H,H) = 10Hz), 8.21 (1H, s), 4.17 (3H, s).

The following steps are based on a synthetic route reported elsewhere.[1]

Compound **2a**:

Yield: 53%

^{1}H-NMR (400MHz, acetone-d6): δ = 9.39 (1H, s), 9.29 (1H, d, ^3J (H,H) = 10Hz), 9.13 (1H, d, ^3J (H,H) = 10Hz), 9.06 (1H, d, ^3J (H,H) = 10Hz), 9.02 (1H, d, ^3J (H,H) = 10Hz), 8.61 (1H, s), 4.90 (6H, m), 4.50 (3H, s). MS (ES-): *m/z* calc. for $C_{23}H_{15}F_9O_{10}S_3$: 717.97; found: 635.20 $[M\text{-}CH_2CF_3]^+$.

Compound **2b**:

Yield: 22%

^{1}H-NMR (400MHz, acetone-d6): δ = 9.44 (1H, s), 9.42 (1H, d, ^3J (H,H) = 10Hz), 9.13 (1H, d, ^3J (H,H) = 10Hz), 9.13 (1H, d, ^3J (H,H) = 7Hz), 9.11 (1H, d, ^3J (H,H) = 7Hz), 8.70 (1H, s), 6.39 (3H, m), 4.51 (3H, s). MS (ES+): *m/z* calc. for $C_{26}H_{12}F_{18}O_{10}S_3$: 921.93; found: 921.84 $[M]^+$.

Compound **2c**:

Yield: 34%

^{1}H-NMR (400MHz, acetone-d6): δ = 9.53 (1H, d, ^3J (H,H) = 10Hz), 9.50 (1H, d, ^3J (H,H) = 10Hz), 9.34 (1H, d, ^3J (H,H) = 10Hz), 9.30 (1H,s), 8.98 (1H, d, ^3J (H,H) = 10Hz), 8.43 (1H, s), 4.41 (3H, s), 3.81 (3H, s), 3.78 (3H, s), 3.77 (3H, s), 2.97 (3H, s) 2.94 (3H, s), 2.93 (3H, s). MS (ES+): *m/z* calc. for $C_{23}H_{27}N_3O_{10}S_3$: 601.09; found: 602.32 $[M+H]^+$.

Compound **2d**:

Yield: could not be determined

^{1}H-NMR (400MHz, acetone-d6): δ = 9.27 (1H, d, ^3J (H,H) = 10Hz), 9.24 (1H, s), 9.12 (1H, d, ^3J (H,H) = 10Hz), 9.03 (1H, d, ^3J (H,H) = 10Hz), 8.88 (1H, d, ^3J (H,H) = 10Hz), 8.42 (1H, s), 4.37 (3H, s), 3.67 (12H, m), 3.48 (12H, m), 3.14 (6H, s) 3.06 (6H, s), 3.05 (6H, s). MS (ES+): *m/z* calc. for $C_{35}H_{51}N_3O_{13}S_3$: 817.26; found: 840.27 $[M+Na]^+$.

Compound **2e**:

Yield: 95%

^{1}H-NMR (400MHz, acetone-d6): δ = 9.34 (1H, d, ^3J (H,H) = 10Hz), 9.22 (1H, d, ^3J (H,H) = 10Hz), 9.19 (1H, s), 9.12 (1H, d, ^3J (H,H) = 10Hz), 9.85 (1H, d, ^3J (H,H) = 10Hz), 8.39 (1H, s), 4.37 (3H, s), 3.75 (6H, m), 3.47 (6H, m), 3.08 (3H, s), 3.07 (3H, s), 3.06 (3H, s). MS (ES+): *m/z* calc. for $C_{26}H_{33}N_3O_{10}S_3$: 643.13; found: 666.38 $[M+Na]^+$.

MPTA:

^{1}H-NMR (400MHz, acetone-d6): δ = 9.44 (1H, d, ^3J (H,H) = 10Hz), 9.35 (1H, d, ^3J (H,H) = 10Hz), 9.21 (1H, d, ^3J (H,H) = 10Hz), 9.19 (1H,s), 8.94 (1H, d, ^3J (H,H) = 10Hz), 8.40 (1H, s), 4.41 (3H, s), 2.94 (3H, s), 2.92 (3H, s), 2.91 (3H, s).

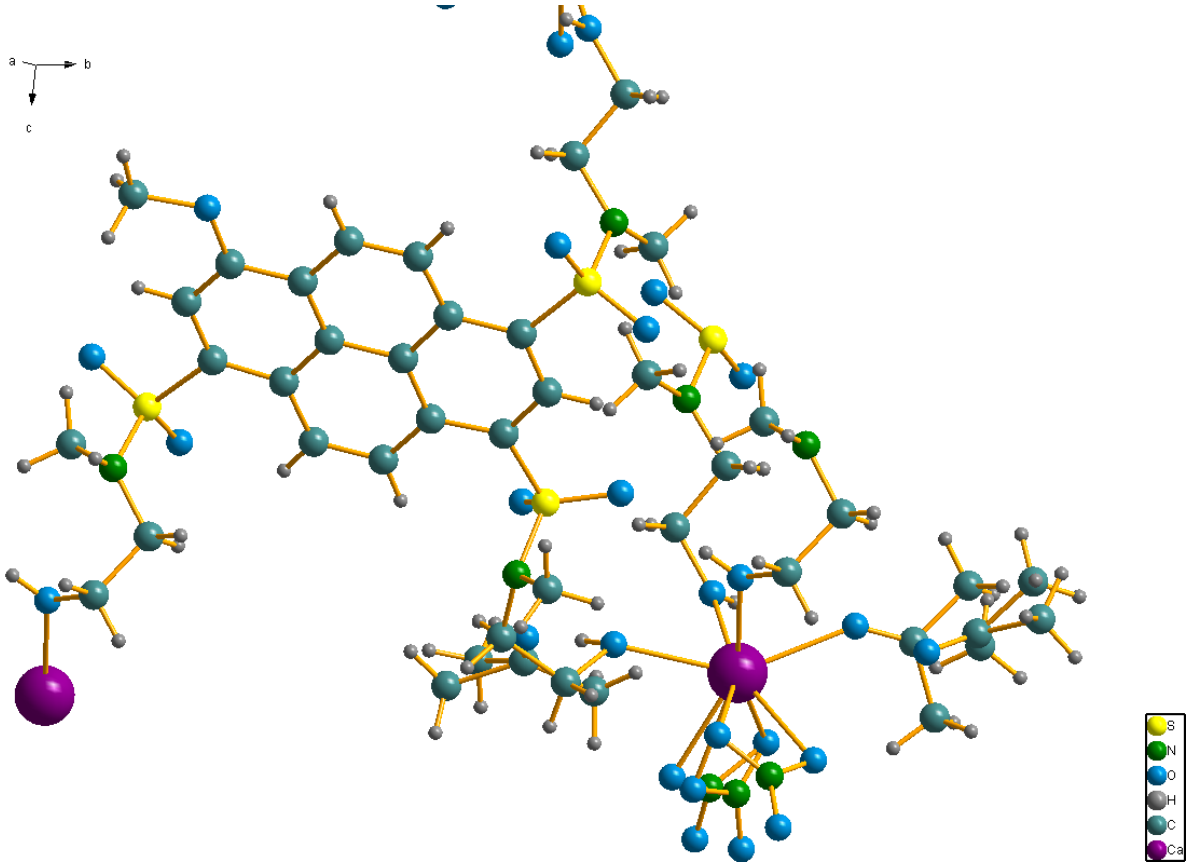

Figure S1. Crystal structure of compound **2e**.

Table 1. Crystal data and structure refinement for **2e**.

Empirical formula	C26 H33 N3 O10 S3 x Ca N2 O6 x 3 C3 H6 O
Formula weight	982.07
Temperature	123(2) K
Wavelength	0.71073 Å
Crystal system	Triclinic
Space group	P-1
Unit cell dimensions	a = 9.9974(6) Å
	b = 13.0768(9) Å
	c = 18.1443(12) Å
Volume	2159.6(2) $Å^3$
Z	2
Density (calculated)	1.510 Mg/m^3
Absorption coefficient	0.374 mm^{-1}
F(000)	1032
Crystal size	0.87 x 0.25 x 0.13 mm^3
Theta range for data collection	1.15 to 26.50°.

Index ranges	-12<=h<=11, -16<=k<=16, -22<=l<=22
Reflections collected	26081
Independent reflections	8729 [R(int) = 0.0381]
Completeness to theta = 26.50°	97.5 %
Absorption correction	None
Max. and min. transmission	0.9530 and 0.7376
Refinement method	Full-matrix least-squares on F^2
Data / restraints / parameters	8729 / 426 / 631
Goodness-of-fit on F^2	1.088
Final R indices [I>2sigma(I)]	R1 = 0.0582, wR2 = 0.1437
R indices (all data)	R1 = 0.0896, wR2 = 0.1609
Largest diff. peak and hole	0.784 and -0.476 e.Å^{-3}

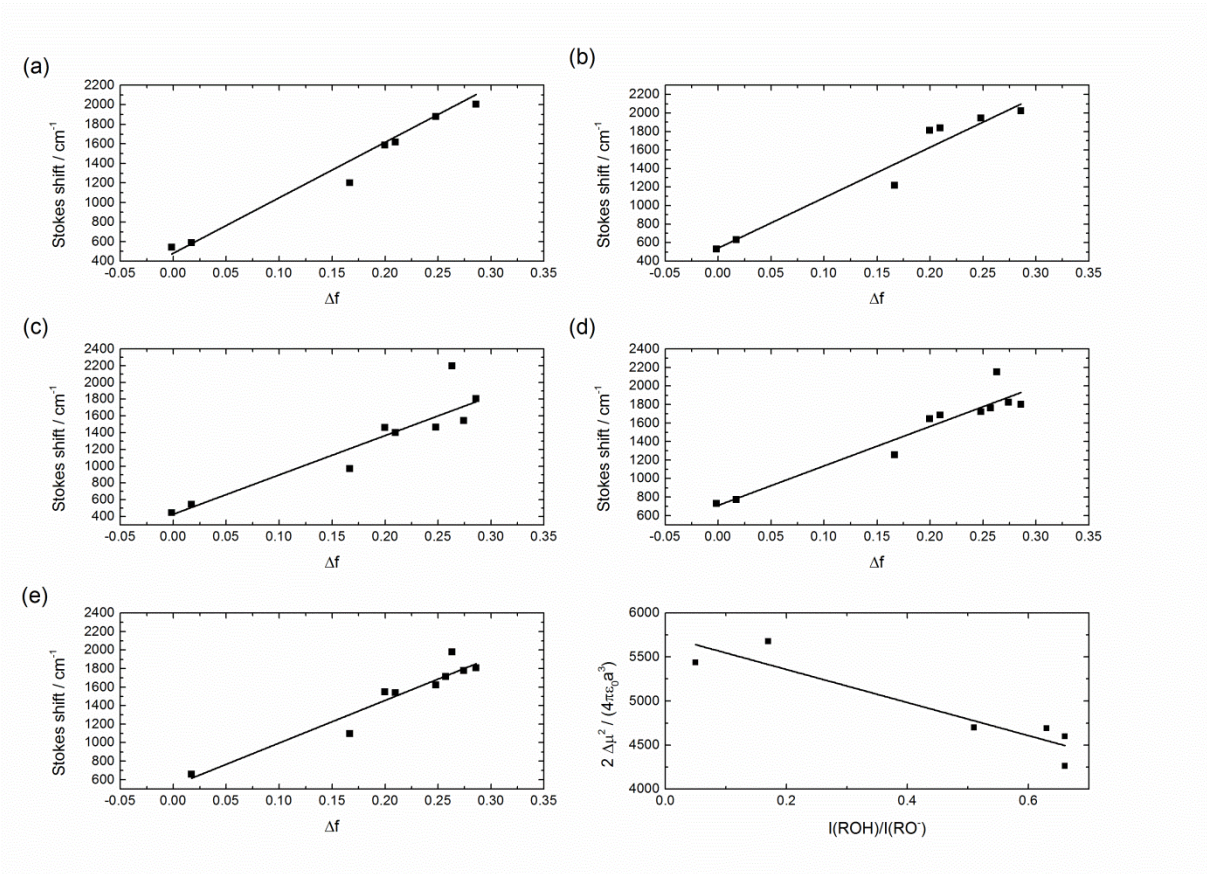

Figure S2. Lippert-Mataga plot of the methylated photoacids in non-acidic solvents. (a) **2a**, (b) **2b**, (c) **2c**, (d) **2d**, ((f)) **2e**, (f) The slope of all Lippert-Mataga plots decreases with decreasing photoacidity (R^2=0.83).

Table S2. The slopes of all Lippert Mataga plots for the methylated compounds. The molecular volume and the calculated change of the dipole moment are also given.

Compound	Slope ($2*(\Delta\mu)^2/(4\pi\varepsilon_0 a^3)$)	a^3 [Å^3]	$\Delta\mu$ [D]
MPTA	4600 (285)	400	13,6
2a	5680 (710)	410	14,5
2b	5440 (490)	511	15,7
2c	4700 (725)	424	13,6
2d	4260 (425)	686	16,4
2e	4600 (490)	480	14,4

Table S3. Kamlet-Taft parameters of the methylated compounds. Standard errors are in parenthesis, R^2 is the correlation coefficient. All values are given in cm^{-1}.

Compound	$\nu_{0,\,abs}$	p_{abs}	a_{abs}	b_{abs}	R^2	$\nu_{0,\,em}$	p_{em}	a_{em}	b_{em}	R^2
MPTA	24040 (30)	-445 (50)	0	0	0.84	23500 (60)	-1870 (100)	-200 (80)	0	0.83
2a	23550 (55)	-475 (65)	0	0	0.64	23045 (130)	-2375 (215)	-200 (80)	0	0.70
2b	23300 (70)	-670 (55)	0	0	0.63	22700 (160)	-2500 (260)	-200 (80)	0	0.61
2c	23750 (45)	-455 (75)	0	0	0.76	23325 (120)	-2110 (200)	-200 (80)	0	0.77
2d	24045 (40)	-435 (65)	0	0	0.81	23300 (95)	-1855 (155)	-200 (80)	0	0.80
2e	23960 (60)	-310 (95)	0	0	0.58	23340 (90)	-1775 (130)	-200 (80)	0	0.78

Table S4. Catalán parameters of the methylated compounds. Standard errors are in parenthesis, R^2 is the correlation coefficient. All values are given in cm^{-1}.

Compound	$\nu_{0,abs}$	Q_{abs}	P_{abs}	A_{abs}	B_{abs}	R^2
MPTA	25075 (60)	-1585 (85)	-210 (20)	-145 (25)	0	0.97
2a	24475 (250)	-1385 (345)	-230 (65)	0	0	0.86
2b	24240 (205)	-1430 (280)	-360 (70)	0	0	0.77
2c	24880 (105)	-1695 (145)	-235 (35)	-240 (45)	0	0.94
2d	25085 (115)	-1565 (155)	-255 (40)	-305 (50)	0	0.93
2e	25070 (75)	-1675 (105)	-145 (25)	-155 (35)	0	0.96
Compound	$\nu_{0,em}$	Q_{em}	P_{em}	A_{em}	B_{em}	R^2
MPTA	24315 (250)	-1305 (355)	-1510 (80)	-350 (95)	0	0.97
2a	25000 (580)	-3130 (800)	-1660 (160)	-505 (205)	0	0.95
2b	24590 (475)	-2975 (655)	-1930 (130)	0	0	0.94
2c	25455 (365)	-3300 (500)	-1590 (100)	-405 (120)	0	0.98
2d	24545 (335)	-2000 (460)	-1410 (90)	-490 (115)	0	0.96
2e	24475 (240)	-1935 (325)	-1265 (75)	-530 (80)	0	0.97

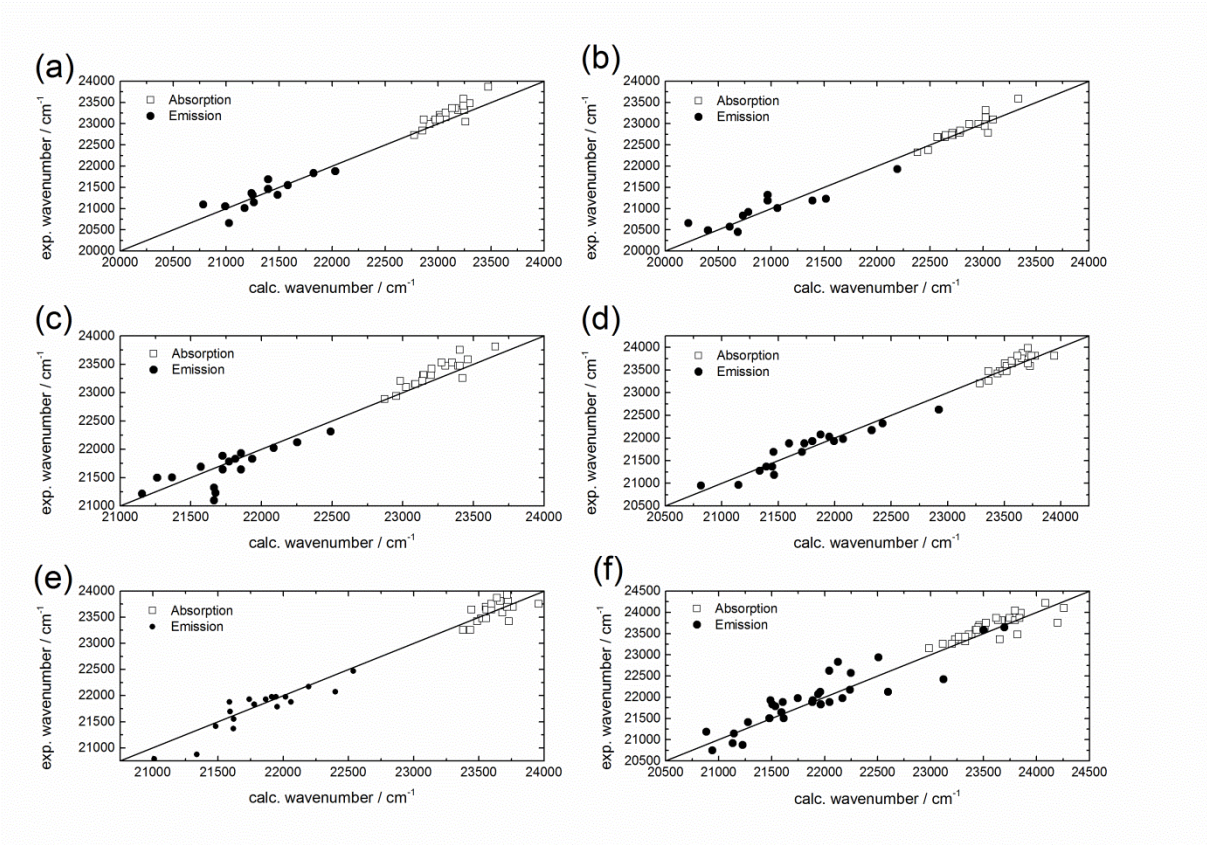

Figure S3. Correlation plots obtained with the Kamlet-Taft analysis of the photoacids. (a) **1a**, (b) **1b**, (c) **1c**, (d) **1d**, (e) **1e**, (f) **HPTA**

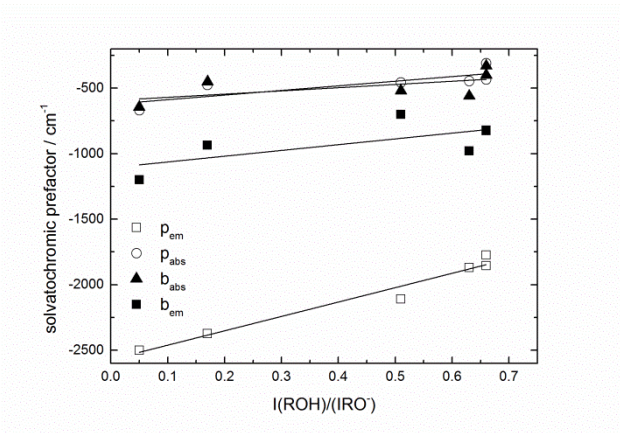

Figure S4. Plot of p_{em} (open squares), p_{abs} (full circles), b_{em} (full squares) and b_{abs} (open triangles) of the photoacids vs. the amount acid fluorescence intensity. The strongest dependence and correlation is observed on p_{em}.

Table S5. Catalán parameters of the photoacids. Standard errors are in parenthesis, R^2 is the correlation coefficient. All values are given in cm^{-1}.

Compound	$\nu_{0,\,abs}$	Q_{abs}	P_{abs}	A_{abs}	B_{abs}	R^2
HPTA	24945 (290)	-1190 (395)	-130 (105)	-240 (140)	-770 (130)	0.67
1a	24725 (340)	-1200 (440)	-585 (110)	0	-585 (140)	0.84
1b	24480 (370)	-1300 (450)	-505 (155)	0	-820 (180)	0.78
1c	25130 (370)	-1695 (465)	-285 (135)	-430 (145)	-780 (155)	0.78
1d	24885 (360)	-1330 (455)	0	-470 (120)	-625 (135)	0.61
1e	25135 (355)	-1755 (450)	0	-385 (120)	-550 (140)	0.57
Compound	$\nu_{0,\,em}$	Q_{em}	P_{em}	A_{em}	B_{em}	**R^2**
HPTA	24900 (620)	-2150 (850)	-1140 (260)	-690 (305)	-1185 (335)	0.82
1a	24765 (1135)	-3255 (1450)	-1040 (205)	0	-1160 (295)	0.87
1b	23290 (700)	-1860 (830)	-930 (240)	0	-1255 (365)	0.87
1c	24660 (475)	-2780 (620)	-705 (145)	-1010 (210)	-890 (185)	0.90
1d	24990 (470)	-3000 (622)	-770 (160)	-995 (235)	-1080 (200)	0.89
1e	26070 (600)	-4400 (760)	-860 (255)	-1040 (280)	-960 (240)	0.80

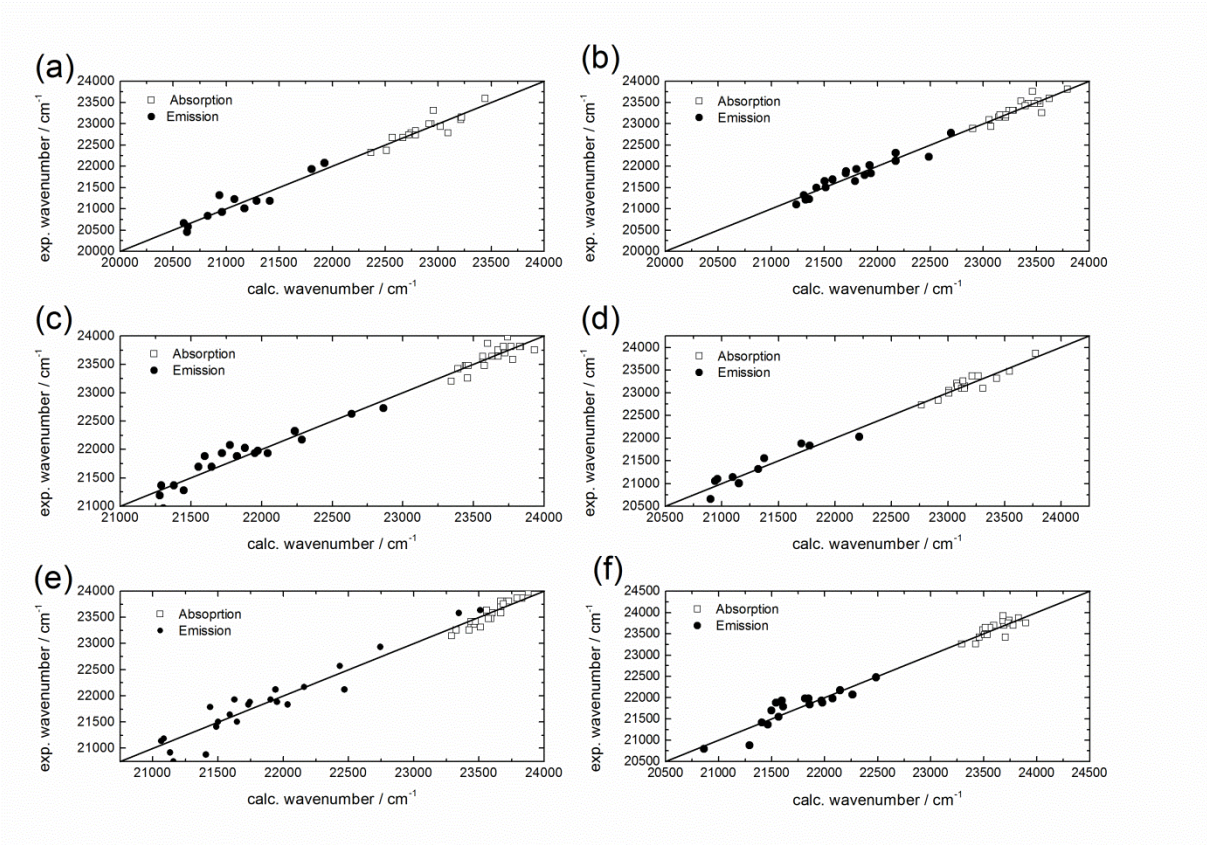

Figure S5. Correlation plots obtained with the Catalán analysis of the photoacids. (a) **1a**, (b) **1b**, (c) **1c**, (d) **1d**, (e) **1e**, (f) **HPTA**

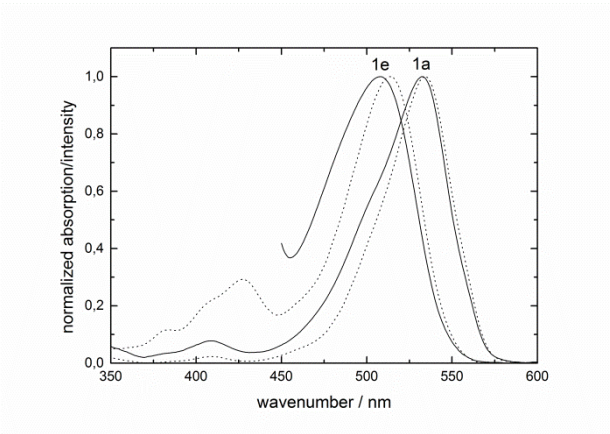

Figure S6. Absorption (full lines) and excitation spectra (dotted lines) of the deprotonated photoacids **1a** and **1e** in ethanol.

Table S6. Catalán parameters of the deprotonated photoacids. Standard errors are in parenthesis, R^2 is the correlation coefficient. All values are given in cm^{-1}.

Compound	$\nu_{0,\,abs}$	A_{abs}	Q_{abs}	R^2	$\nu_{0,\,em}$	A_{em}	Q_{em}	R^2
HPTA	19800 (530)	1955 (190)	-2365 (700)	0.94	18410 (110)	510 (40)	-1025 (150)	0.97
1a	18435 (430)	2260 (170)	-1210 (590)	0.98	18035 (105)	470 (30)	-840 (145)	0.98
1b	18220 (460)	2125 (180)	-1240 (625)	0.98	17990 (170)	400 (50)	-1045 (235)	0.94
1c	20295 (795)	2060 (245)	-3670 (1090)	0.94	18280 (185)	455 (60)	-1260 (255)	0.95
1d	21325 (900)	1875 (240)	-4515 (1265)	0.95	18420 (165)	395 (50)	-1075 (225)	0.95
1e	21295 (1020)	1715 (365)	-3975 (1300)	0.93	18930 (215)	260 (70)	-1570 (280)	0.96

Table S7. . Excited State Properties Predicted by Quantum Chemical Model Calculations for **MPTA** in Acetonitrile (CIS = 16, LE: locally excited, CT: charge transfer)

state	ΔE, eV	λ_{ex}, nm	Δμ, D	*f*	character	Predominant transitions	% contributions
S1	2.99	414	1.52	0.501	LE(Py)	H→L H-1→L+1 H-6→L+5	62 22 10
S2	3.26	381	0.72	0.034	LE(Py)	H-1→L H→L+1	43 50
S3	3.08	402	7.78	0.025	LE CT CT CT	H-4→L+2 H-4→L+3 H-4→L+1 H-4→L+5	62 17 14 10
S4	3.12	398	5.90	0.032	LE+CT LE+ CT CT (Py)	H-2→L+4 H-2→L+3 H-2→L+5	44 36 10
S5	3.14	395	6.14	0.013	CT(Py)+LE CT (Py) LE	H-3→L+3 H-3→L+5 H-2→L+4	48 21 29
S6	3.65	340	0.70	0.003	LE (Py) LE (Py)	H-5→L H→L+6	61 21

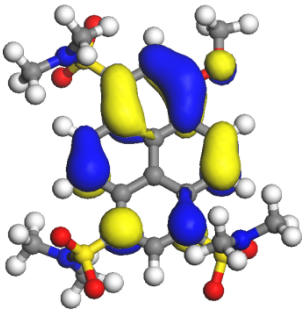	HOMO -9.15 eV	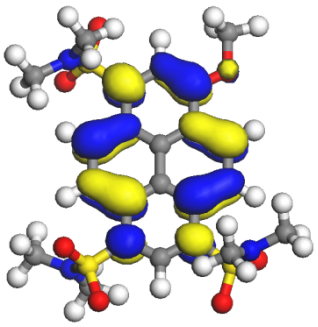	LUMO -2.43 eV
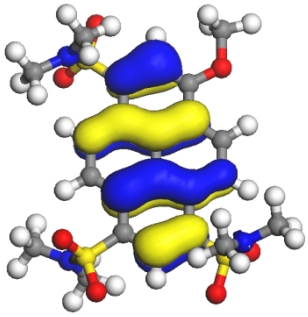	H-1 -10.06 eV	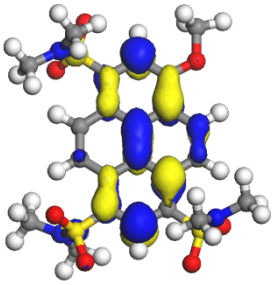	L+1 -1.25 eV
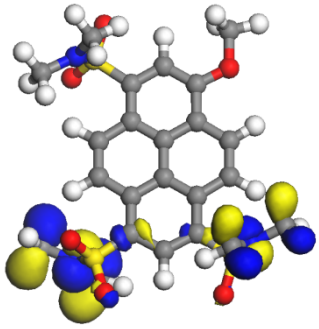	H-2 -10.54 eV	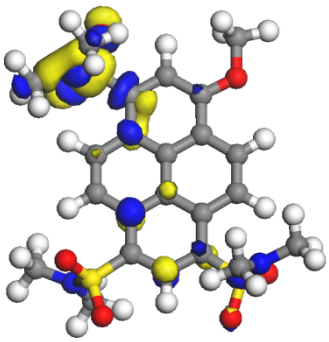	L+2 -1.02 eV
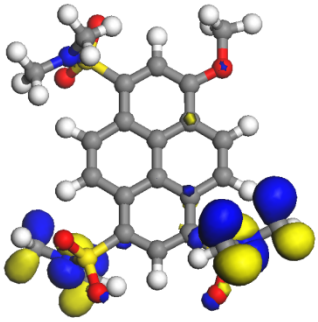	H-3 -10.57 eV	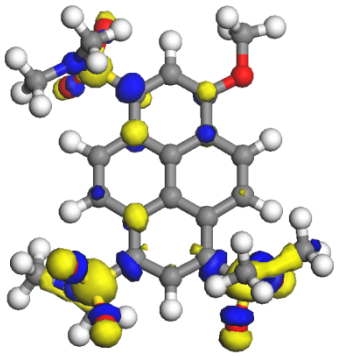	L+3 -0.84 eV

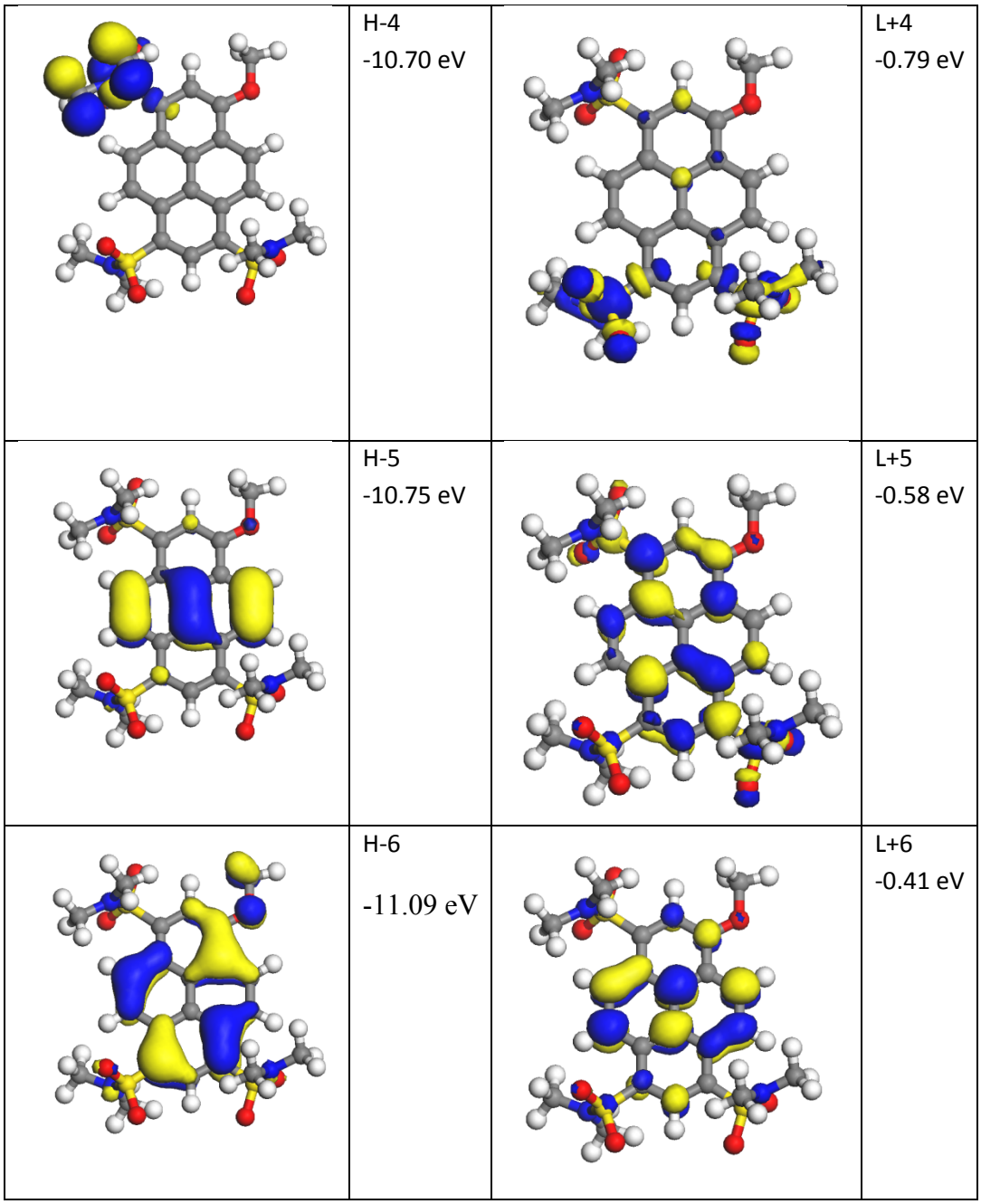

Figure S7. Schematic presentation of the molecular orbitals involved in the CI-description of the excited states of **MPTA** (in acetonitrile).

Table S8. . Excited State Properties Predicted by Quantum Chemical Model Calculations for **MPTS** in Acetonitrile (CIS = 16, LE: locally excited, CT: charge transfer)

state	ΔE, eV	λ_{ex}, nm	Δμ, D	*f*	character	Predominant transitions	%
S1	2.97	416	0.56	0.310	LE (Py)	H→L H-3→L+2	55 13

S2	3.18	389	0.19	0.080	LE (Py)	H-1→L H-3→L+4	45 12
S3	3.86	321	0.31	0.001	LE (Py)	H-2→L H-3→L	58 10
S4	3.91	316	1.11	0.050	LE (Py)	H→L+3 H-3→L+1 H-6→L	42 23 16
S5	4.32	286	0.66	0.009	LE (Py)	H→L+2 H-6→L+1	43 11
S6	4.48	276	3.99	0.565	LE (Py)	H-1→L+1 H-3→L	34 25
S7	4.66	264	3.82	0.755	LE (Py)	H→L+1 H-1→L	43 42

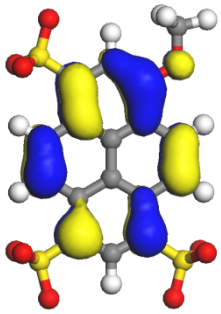	HOMO -8.40 eV	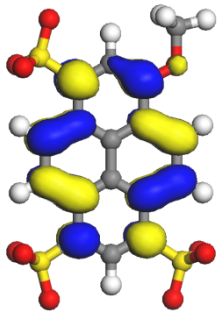	LUMO -1.50 eV
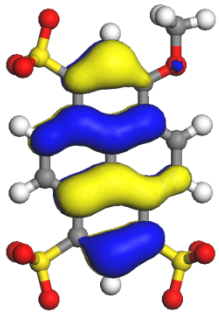	H - 1 -9.25 eV	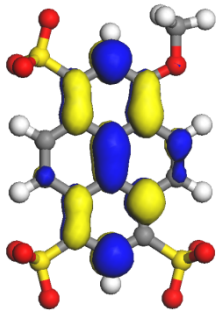	L + 1 -0.50 eV
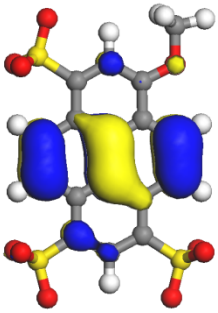	H - 2 -10.11 eV	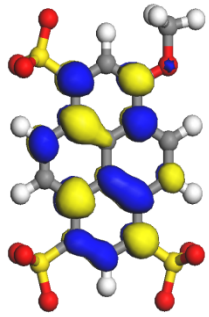	L + 2 0.20 eV

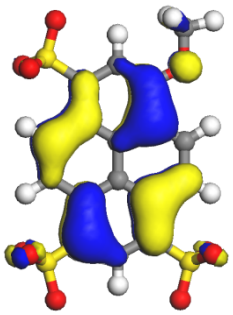	H - 3 -10.28 eV	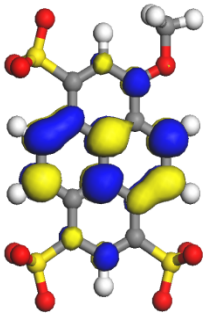	L + 3 0.29 eV
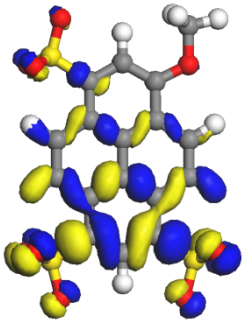	H - 4 -10.66 eV	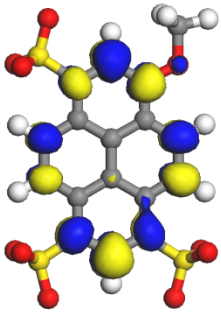	L + 4 0.94 eV
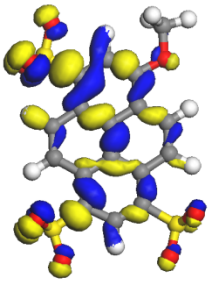	H - 5 -11.05 eV	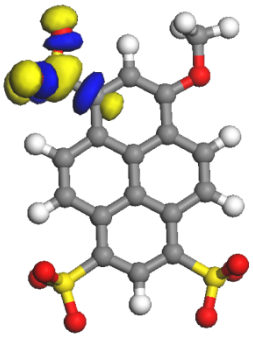	L + 5 1.43 eV
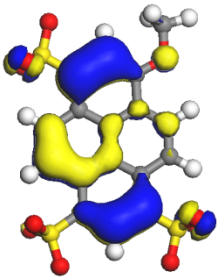	H - 6 -11.17 eV	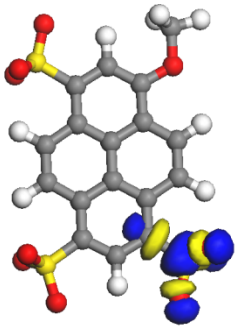	L + 6 1.62 eV

Figure S8. Schematic presentation of the molecular orbitals involved in the CI-description of the excited states of **MPTS** (in acetonitrile).

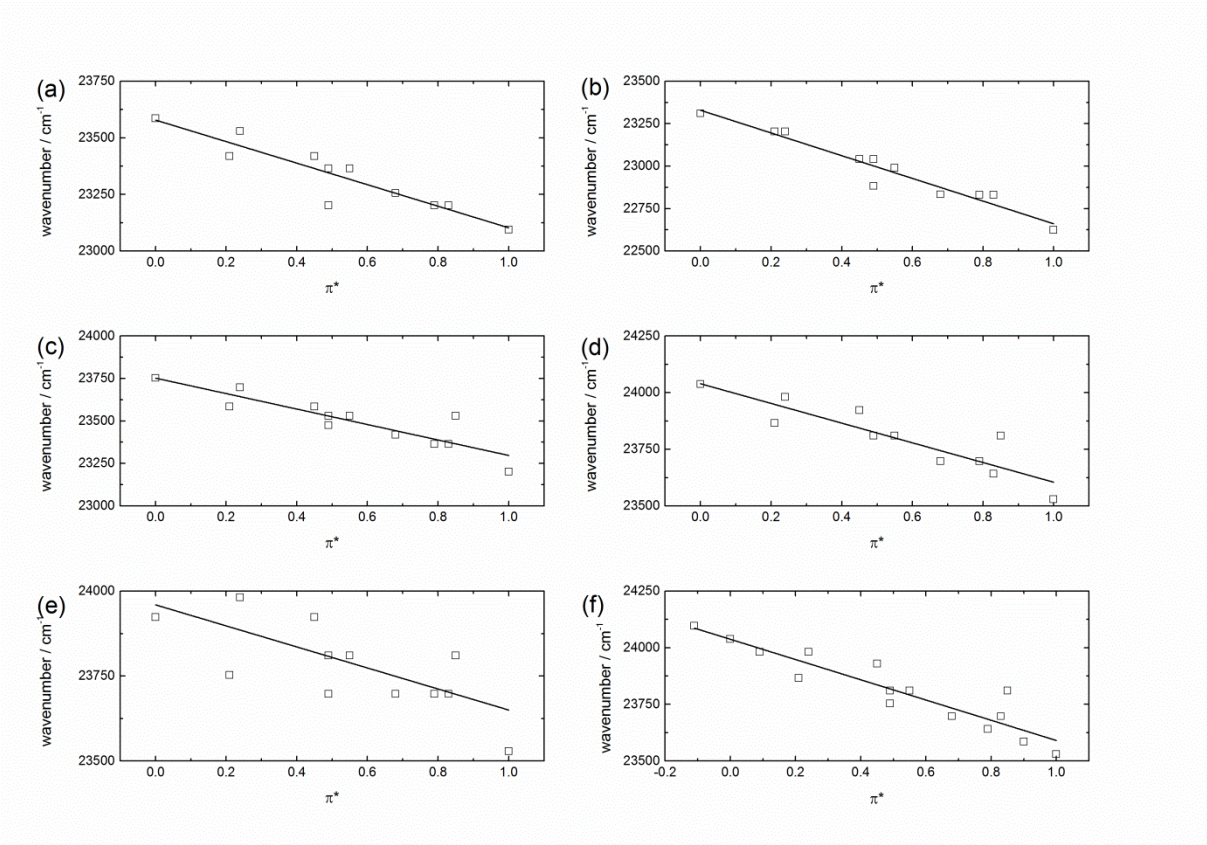

Figure S9. Absorption (squares) frequencies of the methylated photoacids in solvents of increasing polarity. (a) **2a**, (b) **2b**, (c) **2c**, (d) **2d**, (e) **2e**, (f) **MPTA**

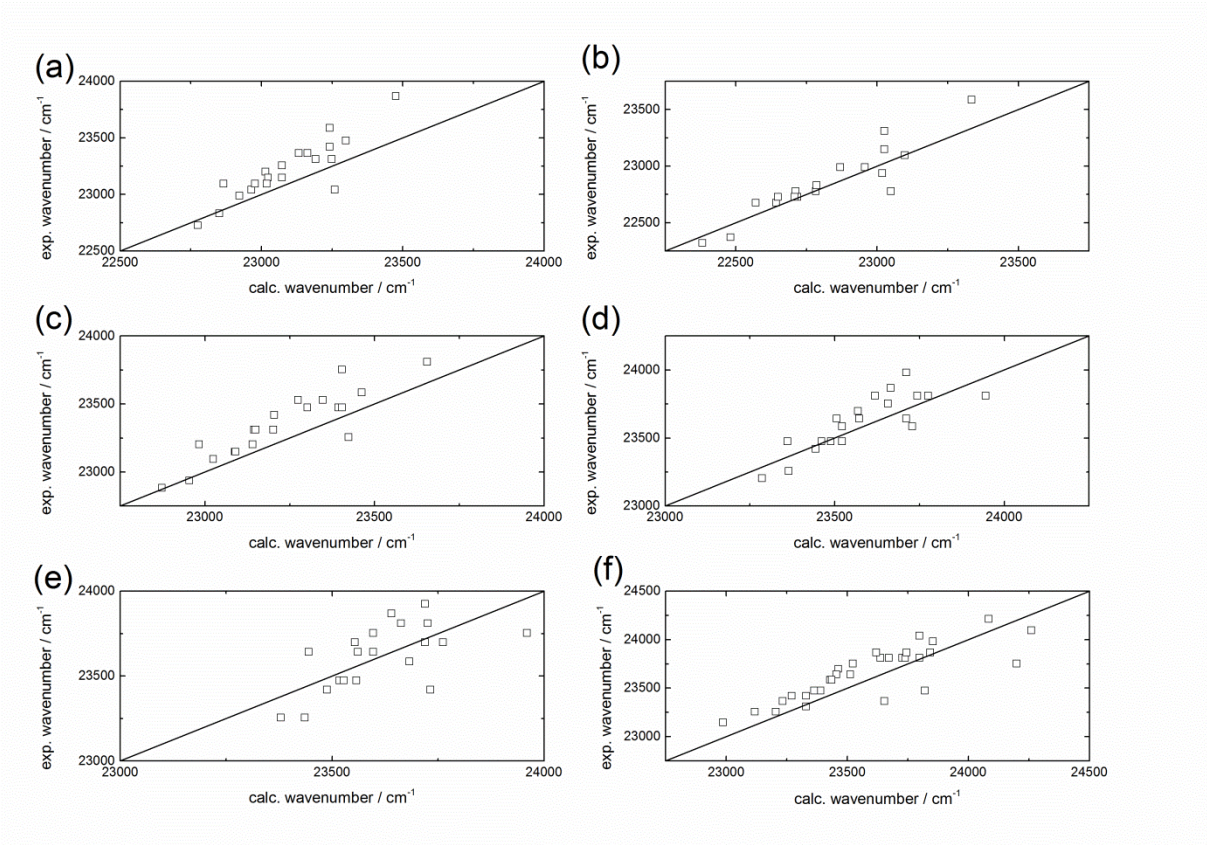

Figure S10. Correlation plots for absorption maxima obtained with the Kamlet-Taft analysis of the photoacids. (a) **1a**, (b) **1b**, (c) **1c**, (d) **1d**, (e) **1e**, (f) **HPTA**

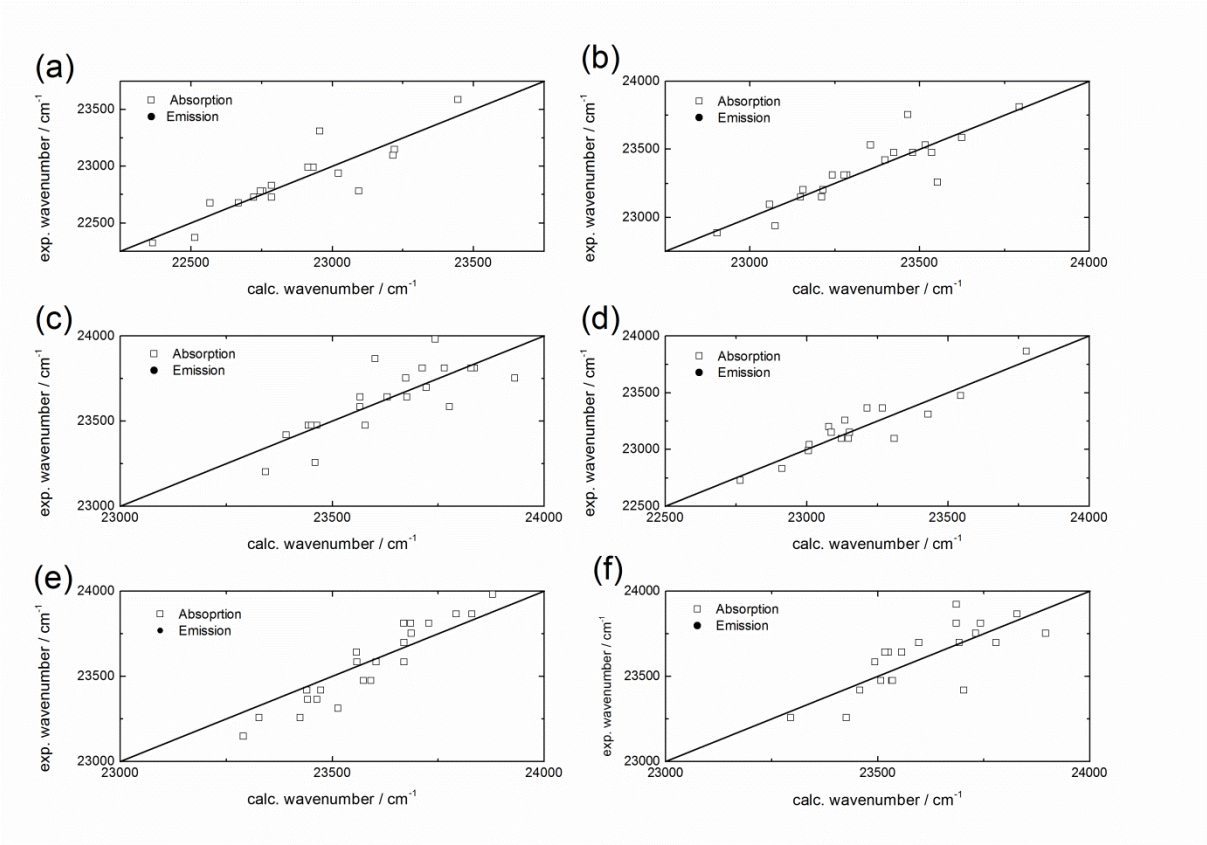

Figure S11. Correlation plots for absorption maxima obtained with the Catalán analysis of the photoacids. (a) **1a**, (b) **1b**, (c) **1c**, (d) **1d**, (e) **1e**, (f) **HPTA**

References

(1) Finkler, B.; Spies, C.; Vester, M.; Jung, G. Versatile Series of Highly Photostable "Super"-Photoacids with High Quantum Yield for Biological and Single-Molecule Investigations. *submitted* **2013** .